RSC Advances

ROYAL SOCIETY OF CHEMISTRY

www.rsc.org/advances

Graphene–hemin hybrid nanosheets as a label-free colorimetric platform for DNA and small molecule assays

Cui Hu, Qiang Xi, Jia Ge, Feng-Yan Luo, Li-Juan Tang, Jian-Hui Jiang and Ru-Qin Yu**

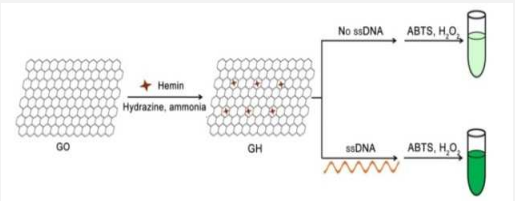

A novel colorimetric platform has been developed for detecting DNA and small molecule based on graphene–hemin hybrid nanosheet in homogenous solution.

Cite this: DOI: 10.1039/c0xx00000x

www.rsc.org/xxxxxx

ARTICLE TYPE

Graphene−hemin hybrid nanosheets as a label-free colorimetric platform for DNA and small molecule assays

Cui Hu, Qiang Xi, Jia Ge, Feng-Yan Luo, Li-Juan Tang*, Jian-Hui Jiang and Ru-Qin Yu*

Received (in XXX, XXX) Xth XXXXXXXXX 20XX, Accepted Xth XXXXXXXXX 20XX
DOI: 10.1039/b000000x

Here we reported a novel label-free colorimetric biosensing strategy based on graphene−hemin hybrid nanosheets (GHs) for DNA and small molecule assays. GHs were synthesized by a simple wet-chemical method and possessed excellent properties of both graphene and hemin. When being mixed with ssDNA, GHs exhibited enhanced catalytic activity in the presence of ABTS and H_2O_2. In contrast, the GHs mixed with dsDNA had lower catalytic activity than that mixed with ssDNA. On the basis of this property of GHs, a novel universal label-free colorimetric method was proposed. This simple strategy owns the merits over conventional assays in its label-free design, extreme operation simplicity and low cost. DNA and cocaine were studied as model cases and the results revealed the developed method had a potential of becoming a universal platform for detection of a wide range of analytes.

Introduction

Recently, the appearance of a new hybrid nanosheet consisting of graphene oxide (GO) and hemin has attracted research interests in the field of biochemical sensing.[1−5] As a one-atom-thick nanomaterial, GO has attracted much attention for its excellent physical properties, such as large surface area, good water-solubility and the ability of distinguishing single-strand DNA (ssDNA) from double-strand DNA (dsDNA).[6−8] Especially, its fluorescence quenching ability for fluorophores is also superior to many other materials, which has made it one of the most commonly used nanomaterial for fluorescence biosensing in the last decade.[9−11] However, the fluorescence methods are usually associated with disadvantages such as complicated labelling and high cost. Hemin (iron protoporphyrin), as the active center of heme-proteins, has the peroxidase-like activity similar to the peroxidase enzyme, which could provide a colorimetric signal.[12,13] Therefore, the graphene−hemin hybrid (GHs) possesses both excellent properties of graphene and hemin. Many researches that focused on the catalytic performance of GHs have been conducted.[14-19] For example, hemin functionalized GO has served as peroxidase probe for sensitive detection of biomarkers,[15-17] effective oxygen reduction catalyst for oxidation of C-H bond in organic compounds [18] and sensitive quenching of fluorescent material.[19] Thus, this novel nanomaterial is expected to offer new thoughts for the application in the field of application.

Cocaine is one of the most dangerous and illegally abused drugs, due to its enormous impact to the central nervous system and human's health, the sensitive and selective methods have been developed for many years for determination of cocaine.[20−22]Since the aptamer of cocaine was discovered in 2000, a number of sensors based on cocaine aptamer have been reported.[23,24] Various amplification strategies have been applied in these methods for improving the sensitivity, such as rolling circle amplification (RCA), polymerase chain reaction (PCR) and so on.[25−28] However, in most cases, the amplification strategies have their limitations owing to the sophisticated instrumentation, high technical expertise requirement , as well as long analysis time. Therefore, it is of considerable interest to synthesize new materials possessing both peroxidase activity and DNA recognition ability in cocaine assay.

In this paper, GH nanosheets were synthesized through simple wet-chemical method, which were firstly found responsive to ssDNA and able to distinguish ssDNA and dsDNA directly in the presence of 2,2'-azinobis-(3-ethylbenzthiazoline)-6-sulphonate (ABTS) and H_2O_2. When ssDNA was mixed with the GHs, the colorimetric signal intensity was increased significantly. In contrast, the GHs mixed with dsDNA had lower catalytic activity than that with the ssDNA counterparts. Compared with previous report, the ability to distinguish ssDNA and dsDNA of GHs didn't need salt and the whole reaction process was homogeneous.[1] Based on this finding, we proposed a novel label-free colorimetric strategy and constructed sensors for DNA and cocaine assay. Moreover, this proposed strategy had the potential to be practical due to its extreme simplicity and low cost.

Experimental section

Reagents

Graphene oxide was purchased from XF Nano Co. Ltd (Nanjing, China). Hemin, ABTS, TMB (3,3',5,5'-tetramethylbenzidine) and hydrazine hydrate solution were obtained from Sigma-Aldrich (Missouri, USA). Cocaine, morphine hydrochloride (MHC), caffeine and theophylline were obtained from Beijing Institute for Drug Control (Beijing, China) and used without further purification. O-phenylenediamine (OPD), H_2O_2 and $NH_3{\bullet}H_2O$ were supplied by Sinopharm Chemical Reagent Co. Ltd (Shanghai, China). DNA oligonucleotides were obtained from Sangon Biotechnology Co. Ltd (Shanghai, China). The DNA sequences were as follow:

P1 (Probe):

ACCTGGGGGAGTATTGCGGAGGAAGGTTTTTT

T1 (Complementary target):
AAAAAACCTTCCTCCGCAATACTCCCCCAGGT

T2 (Single base mismatch target):
AAAAAACCTTCCTCCGCAATACTCCCCCAGCT

T3 (Three bases mismatch target):
ATAAAACCTTCCTCAGCAATACTCCCCCAGCT

T4 (Unrelated DNA):
AGTCCGTGGTAGGGCAGGTTGGGGTGACTAGT

P2 (Cocaine aptamer):

GGGAGACAAGGAAAATCCTTCAATGAAGTGGGTCTCCC

Deionized and sterilized water (resistance > 18.2 MΩ cm^{-1}) was used throughout the experiments.

Apparatus

AFM images were taken through a multimode 8 atomic force microscope (Bruker, USA) and the surface was scanned at 1 Hz with the resolution of 512 lines/image. TEM images were obtained with a JEM−2100F high-resolution transmission electron microscope operating at 200 kV. Kinetic measurements were carried out by monitoring the absorbance at corresponding wavelength on a Shimadzu UV−2450 UV−Vis spectrophotometer.

Preparation of hemin functionalized graphene nanosheets (GHs)

GH nanosheets were synthesized according to the previously reported procedure.[1] Hemin was assembled on the surface of graphene oxide sheets via π-π interaction between the porphyrin ring and the hexagonal cells of the graphene oxide. The homogenous graphene oxide (20.0 mL of 0.5 mg/mL dispersion) was mixed with 20.0 mL of 0.5 mg/mL hemin followed by drastic shaking for several minutes. Then 200.0 μL ammonia solution and 30.0 μL hydrazine hydrate were added to the solution. After being vigorously shaken for 1 h, the vial was put in a water bath (60 °C) for 24 h. The obtained black dispersion was then centrifuged at 13,000 rpm for 30 min to remove free hemin and the precipitated conjugates were redispersed in water followed by rinsing with water for three times. The acquired GHs could be redispersed in water to a final concentration of 10 μg/mL. Moreover, the graphene oxide nanosheets were treated under identical conditions except no hemin was added, which obtained reduced graphene oxide (RGO).

Investigation of the peroxidase-like activity of GHs

Firstly, GHs solution (20 μL, 5 μg/mL) was added in 60 μL PB buffer (125 mM, pH 5.0). Then 10 μL of ABTS (50 mM) and 10 μL of H_2O_2 (100 mM) were added, so does the substrate of TMB (10 mM) and OPD (10 mM). Kinetic measurements were carried out immediately by monitoring the absorbance at 420 nm, 652 nm and 450 nm accordingly on a Shimadzu UV−2450 UV−Vis spectrophotometer. In contrast, the same color reaction was performed in the presence of reduced graphene oxide (RGO).

Response to ssDNA of GHs

Different concentration of P1 (10 μL) and the GHs solution (10 μL, 10 μg/mL) were mixed in 60 μL of PB buffer (125 mM, pH 5.0) incubating for 10 min. Then 10 μL of ABTS (10 mM) and 10 μL of H_2O_2 (200 mM) were added. Kinetic measurements were carried out immediately by monitoring the absorbance at 420 nm on a Shimadzu UV−2450 UV−Vis spectrophotometer.

Ability to distinguish ssDNA and dsDNA of GHs

P1 was hybridized with T1 through annealing in Tris-HCl buffer (10 mM, pH 7.9) to obtain 2 μM dsDNA. Then P1 (2 μM, 10 μL) and the obtained dsDNA (2 μM, 10 μL) was respectively mixed with GHs solution (10 μL, 10 μg/mL) in 60 μL PB buffer (125 mM, pH 5.0) incubating for 10 min. Finally, 10 μL of ABTS (10 mM) and 10 μL of H_2O_2 (200 mM) were added. Kinetic measurements were carried out as above mentioned.

Label-free colorimetric assay based on GHs for DNA

The P1 (2 μM, 10 μL) was mixed with 10 μL of target DNA (T1) in 50 μL of buffer solution (50 mM NaH_2PO_4, pH 5.0) at 37 °C for 1h; then 10 μL of GHs (10 μg/mL) was added into the reaction buffer incubating for 10 min; finally 10 μL of ABTS (10 mM) and 10 μL of H_2O_2 (200 mM) were added followed immediately by kinetic measurements.

Label-free colorimetric assay based on GHs for cocaine

The assay procedures could be described as follows: the cocaine aptamer P2 (500 nM,10 μL) was mixed with 10 μL of cocaine sample in 50 μL of buffer solution (50 mM NaH_2PO_4, pH 3.6) at 37 °C for 1h; then 10 μL of GHs (10 μg/mL) was added into the reaction buffer incubating for 10 min; finally 10 μL of ABTS (5 mM) and 10 μL of H_2O_2 (100 mM) were added followed immediately by kinetic measurements.

Results and discussion

Characterization of GHs

We prepared the graphene−hemin nanosheet through the π-π interaction. This nanocomposite could be obtained via mixing the graphene oxide suspension with hemin by hydrazine and ammonia reduction as illustrated in Scheme 1. The preparation of GHs was characterized by UV−Vis spectra. The GO dispersion displayed a maximum absorption at 227 nm corresponding to the π−π* transition of aromatic C=C bond and a shoulder at 290−300 nm which was attributed to the n−π* transition of the C=O

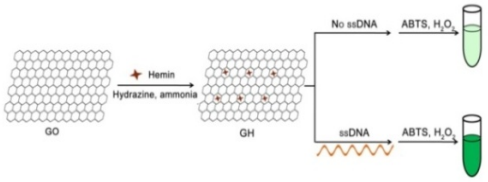

Scheme 1. The preparation and response to DNA of GHs.

bond.[29] The spectrum of hemin solution exhibited a strong peak at 388 nm attributed to the Soret band of porphyrin. Once reduced, the GHs contained two characteristic absorption peaks at 265 nm and 418 nm. The absorption peak at about 265 nm was corresponding with the reduced graphene oxygen (RGO), which was 38 nm red shift compared to GO while the characteristic absorption at 418 nm was attributed to the Soret band of hemin with 30 nm red shift. Remarkably, the graphene dispersion without hemin functioned displayed only an absorption peak at 264 nm and the shoulder peak at 290−300 nm correlated to the

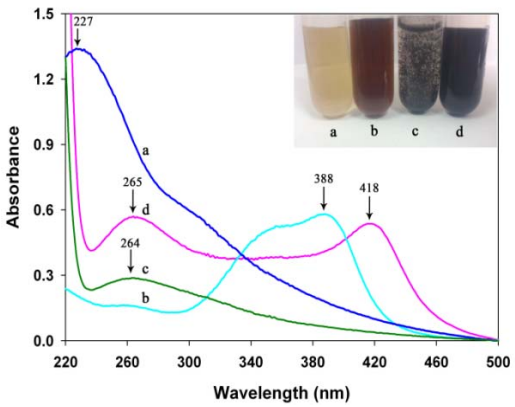

Figure 1. UV−Vis spectra of GO suspension(a), hemin solution (b), RGO suspension (c) and GHs suspension (d). Inset: photographs of GO (0.5 mg/mL) (a), hemin (0.5 mg/mL) (b), RGO (0.25 mg/mL) (c) and GHs (200 μg/mL) (d).

C=O bond disappeared. These observations indicated the occurrence of the strong π−π stacking interactions between the RGO and hemin, resulting in the formation of GHs. In addition, the GHs dispersion solution was stable and no precipitation was observed after being kept for several months (inset d in Figure 1), while the graphene dispersion without hemin congregated quickly (inset c in Figure 1). These results demonstrated that hemin molecules could protect the reduced graphene oxide and made it stable.

AFM was also used to observe the morphology and thickness of GH. The thickness of RGO was about 0.69 nm (Figure 2A, C) corresponding to previously reported single-layer exfoliated sheets.[30] While the thickness of GH was about 1.19 nm (Figure 2B, D), which showed a 0.5 nm increase in height after functioning with hemin. This was in agreement with the previous report and the GHs was deemed obtained accordingly.[1] The formation of GHs was also characterized by TEM. Figure S1A indicated that there was nothing attached to the graphene nanosheet. However, the nanosheet being covered with small particles was obviously observed in S1B, which was regarded as hemin. Considering the AFM and TEM data, we assumed that the reduced graphene nanosheets were covered by a monolayer hemin.

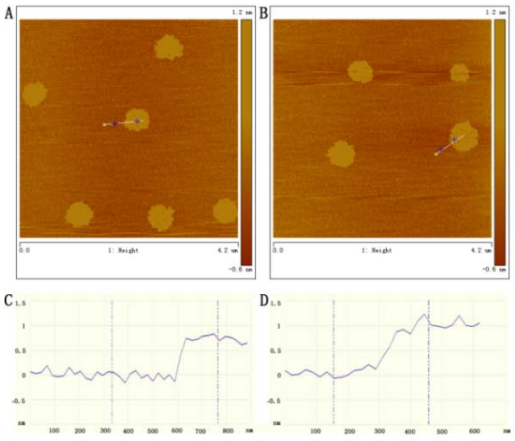

Figure 2. AFM images and height profiles of RGO (A, C) and GH (B, D).

Peroxidase-like Activity of GHs.

It is well known that hemin is the activate site of peroxidase enzyme and exhibits the peroxidase-like activity similar to the peroxidase enzyme. Hence the GHs were supposed to have the peroxidase-like activity. We investigated the catalytic oxidation reaction of GHs and RGO in the presence of different peroxidase substrates such as ABTS, TMB, and OPD; in the presence of H_2O_2 and substrate, the color change was monitored by the absorbance changes at 420 nm (ABTS), 652 nm (TMB) and 450 nm (OPD) respectively. As shown in Figure S2A, the GHs (b) catalyzed a large absorbance change, while only slight change was observed in the presence of RGO (a). The similar phenomena were both observed when selecting TMB and OPD as substrates as illustrated in Figure S2B and S2C. These observations indicated that GHs exhibited peroxidase-like activity while the activity of RGO was much less, demonstrating that hemin served as a catalyst similar to the peroxidase enzyme.

Response to ssDNA and distinguishing ssDNA from dsDNA

For GHs, we found that they have the ability of responding to ssDNA in the presence of ABTS and H_2O_2 as shown in Scheme 1. It was observed that when P1 was mixed with the GHs, the colorimetric signal intensity was increased significantly. Figure 3A shows that the GHs mixed with 200 nM P1 displayed much higher peroxidase-like activity than GHs even in substrate of low concentration and buffer with unsuitable pH. And with the concentration of P1 increased, the oxidation product of ABTS showed higher absorbance signal as illustrated in Figure 3A. Previous reports demonstrated many aromatic compounds can be stacked on DNA to some extent via π-π interaction.[31,32] Therefore, the mechanism of such a phenomenon was presumed to be that ssDNAs absorbed by hemin-rGO hybrid nanosheets have the ability of stacking ABTS and increasing its local concentration on the surface of hemin-rGO, which can, thus, lead to improved catalytic efficiency of hemin-rGO as well as enhanced UV-Vis signal of the reaction system. To confirm this hypothesis, we further investigated whether the GHs could distinguish between ssDNA and dsDNA. Figure 3B shows that GHs mixed with the hybrid of P1 and T1 had lower catalytic activity than that mixed with P1, which indicated that GHs had the ability of distinguishing ssDNA from dsDNA directly. Compared with traditional strategies associated with graphene, this phenomenon was novel and made the as-prepared GHs an ideal nanocomposite used in colorimetric sensors.

GHs-based biosensor for DNA assay

Based on this unique property of GHs, we assumed that this material could be applied in detection of DNA. It was well known that sensitive detection of nucleic acids had widespread applications in gene expression and clinical disease diagnostics.[33,34] Thus, strategies for sensitive and selective detection of DNA were an urgent need. Figure 4A illustrates the analytical principle of the biosensor for DNA assay. First, a complementary DNA (P1) of the target DNA (T1) was introduced as a probe. In the absence of target DNA, the catalytic activity and signal intensity would be high owing to the existence of ssDNA. When adding the target DNA, the ssDNA was turned into dsDNA through hybridization and the absorbance signal would be significantly lower.

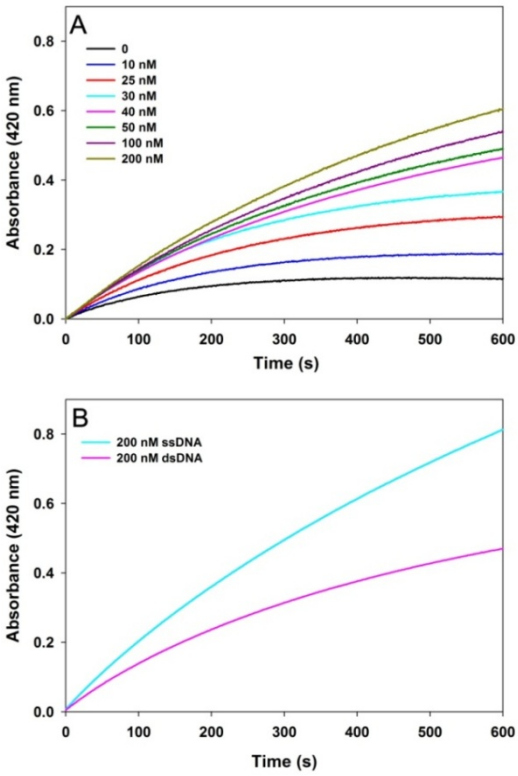

Figure 3. A) Time-dependent absorbance changes at 420 nm in the presence of different amounts of P1 ranging from 0 to 200 nM (0, 10, 25, 30, 40, 50, 100, 200 nM). B) Time-dependent absorbance changes at 420 nm in the presence of 200 nM ssDNA and dsDNA.

Then we investigated the concentration dependence with the target DNA. The concentration of the probe was chosen as 200 nM. The concentrations of GHs, ABTS and H_2O_2 were 1 μg/mL, 1 mM and 20 mM, respectively. Figure 4B depicts kinetic spectroscopy in the presence of different amounts of target DNA (0, 10, 20, 30, 50, 200 nM). A gradual decrease in absorbance at 10 min was observed with the increasing concentration of DNA target. Figure 4C displays the relationship between the absorbance and different target DNA concentrations after an interval of 10 min. A linear relationship was observed between the absorbance and different target DNA concentrations with a correlation coefficient R^2=0.9970. The calibration equation is A=0.6736−0.0025C, where A is the absorbance and C refers to the DNA concentration. In terms of the 3σ rule, the detection limit was estimated to be 9 nM.

Furthermore, control experiments using T2 (single base mismatch), T3 (three bases mismatch) or T4 (unrelated DNA) were performed to investigate the specificity of the proposed strategy. As illustrated in Figure S3A, the absorbance ratios were much lower (A_0/A) in the presence of the non-complementary sequences compared with the target one, implying the proposed sensor strategy had desirable selectivity and thus providing a simple but specific platform for DNA assays.

GHs-based biosensor for small molecule assay

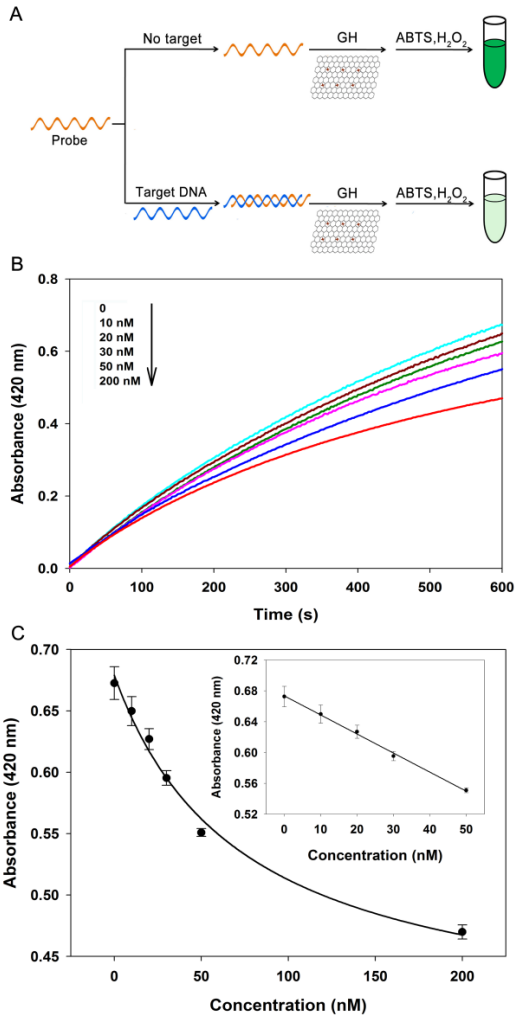

Figure 4. A) Schematic illustration of procedures for DNA detection. B) Time-dependent absorbance changes at 420 nm in the presence of different amounts of target DNA (0, 10, 20, 30, 50, 200 nM). C) Calibration curve corresponding to the absorbance for varying concentrations of target DNA with an intervening time of 10 min. Inset shows a linear calibration curve from 10 to 50 nM. The error bars represent the standard deviation of three experiments.

After observing the colorimetric assay was effective for DNA, we supposed that a nucleic acid aptamer could be used as a DNA probe to detect corresponding target such as protein or small molecules. Due to the enormous impact to human's health of cocaine, cocaine was chosen as a model analyte to develop a label-free colorimetric biosensor.

The protocol of our method is shown in Figure 5A. First, cocaine aptamer P2 was serving as a probe. In the absence of the target, the mixture catalyzed a great absorption change of ABTS with the adding of H_2O_2. However, when adding cocaine, the absorbance change was greatly decreased. With the optimization of experimental conditions, we finally choose 50 nM as the probe concentration. The optimal pH was 3.6 and the concentrations of GHs, ABTS and H_2O_2 were 1 μg/mL, 0.5 mM and 10 mM, respectively. As shown in Figure 5B, in the absence of cocaine, the absorbance at 420 nm was almost 2-fold as that with 50 mM cocaine being present after 10 minutes reaction, which demonstrated the feasibility of the proposal.

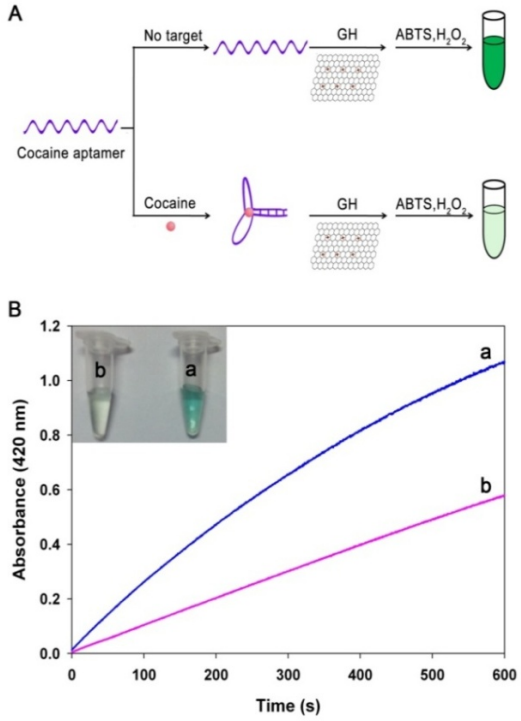

Figure 5. A) Schematic illustration of procedures for cocaine detection. B) Time-dependent absorbance changes at 420 nm in the absence of cocaine (a) and in the presence of cocaine (b, 50 mM).

Next, the effect of concentration of the target cocaine was investigated. Figure 6A displays time-dependent absorbance changes in the presence of different amounts of target cocaine. As shown in Figure 6A, a gradual decrease in absorbance at 10 min was observed with the increasing concentration of cocaine and a dynamic range from 0 to 50 mM. Figure 6B depicts the relationship between the absorbance and different cocaine concentrations after an interval of 10 min. The assay exhibited a linear correlation in the concentration ranging from 500 μM to 5 mM. The calibration equation is A=1.112−0.04978C, where A is the absorbance and C refers to the cocaine concentration. The corresponding correlation coefficient of the calibration curve is 0.9922. The detection limit was estimated to be 230 μM according to the 3σ rule.

Further investigation of the specificity of the sensor was performed. Three typical interfering compounds were chosen as controls: caffeine, theophylline and morphine hydrochloride (MHC). As illustrated in Figure S4A, nearly coincident kinetic data were observed in the addition of caffeine, theophylline and MHC (5 mM) compared with the blank, while the absorbance was decreased to a certain degree after 10 mins reaction by the addition of cocaine (5 mM). This result demonstrated that the biosensor had selectivity for cocaine. Additionally, the developed biosensor was able to detect other analytes by employing additional aptamers.

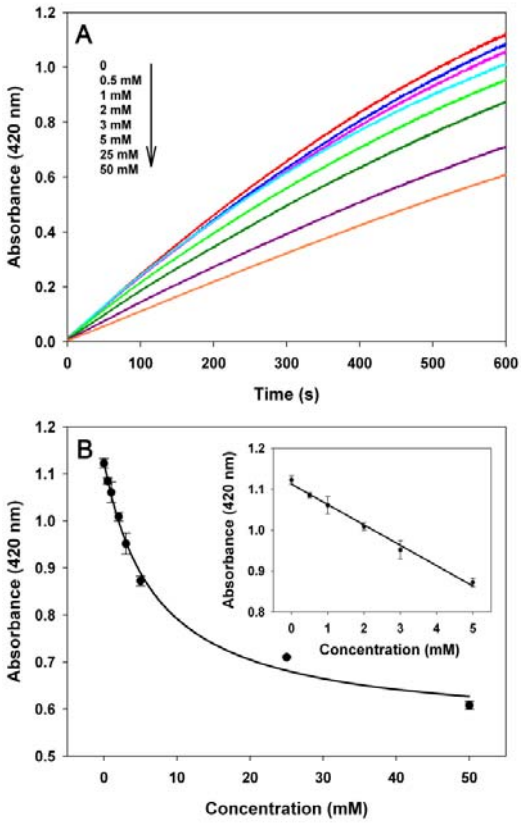

Figure 6. A) Time-dependent absorbance changes at 420 nm in the presence of different amounts of cocaine ranging from 0 to 50 mM (0, 0.5, 1, 2, 3, 5, 25, 50 mM). B) Calibration curve corresponding to the absorbance for various concentrations of cocaine with an intervening time of 10 min. Inset shows a linear calibration curve from 0.5 to 5 mM. The error bars represent the standard deviation of three experiments.

Conclusion

In summary, we have prepared hemin−graphene hybrid nanosheets which possess desirable water-solubility and stability. Especially, it is found that the GHs have peroxidase-like activity and the ability to identify ssDNA and dsDNA. Based on the special properties of the GHs, we have proposed a universal label-free colorimetric sensing strategy for DNA and cocaine assays. The proposed method showed the advantages including operation simplicity, low cost and label-free design. Via changing the sequence of DNA or using different aptamers, the proposed strategy has a potential to be a universal platform for the detection of various analytes including protein, DNA and small molecules.

Acknowledgments

This work was supported by NSFC (21025521, 21205034, 21035001, 21190041, 91317312), Doctoral Fund of Ministry of Education of China (New Teachers, 20120161120032), Hunan Provincial NSFC (13JJ4031). We also thank Meng-Meng Guo for her contribution in correcting the language of the manuscript.

Notes and references

State Key Laboratory of Chemo/Bio–Sensing and Chemometrics, College of Chemistry and Chemical Engineering, Hunan University, Changsha, 410082, P. R. China. E-mail: tanglijuan@hnu.edu.cn; rqyu@hnu.edu.cn. Tel.: 86-731-88822577; Fax: 86-731-88822577.

1 Y. J. Guo, L. Deng, J. Li, S. J. Guo, E. K. Wang and S. J. Dong, *ACS Nano*, **2011**, 5, 1282.
2 Y. Tao, Y. H. Lin, J. S. Ren and X. G. Qu, *Biomaterials*, **2013**, 34, 4810.
3 T. Xue, S. Jiang, Y. Q. Qu, Q. Su, R. Cheng, S. Dubin, C. Y. Chiu, R. Kaner, Y. Huang and X. F. Duan, *Angew. Chem. Int. Ed.*, **2012**, 51, 3822.
4 B. Lin, Q. Q. Sun, K. Liu, D. Q. Lu, Y. Fu, Z. A. Xu and W. Zhang, *Langmuir*, **2014**, 30, 2144.
5 W. Wei, D. M. Zhang, L. H. Yin, Y. P. Pu and S. Q. Liu, *Spectrochim. Acta A*, **2013**, 106, 163.
6 C. N. R. Rao, A. K. Sood, K. S. Subrahmanyam and A. Govindaraj, *Angew. Chem. Int. Ed.*, **2009**, 48, 7752.
7 Y. X. Xu, H. Bai, G. W. Lu, C. Li, and G. Q. Shi, *J. Am. Chem. Soc.*, **2008**, 130, 5856.
8 S. J. Liu, Q. Wen, L. J. Tang and J. H. Jiang, *Anal. Chem.*, **2012**, 84, 5944.
9 X. Q. Liu, R. Aizen, R. Freeman, O. Yehezkeli and I. Willner, *ACS Nano*, **2012**, 6, 3553.
10 J. Z, M. J. Tao and Y. Jin, *Analyst*, **2014**, 139, 3455.
11 Z. S. Qian, X. Y. Shan, L. J. Chai, J. J. Ma, J. R. Chen and H. Feng, *Nanoscale*, **2014**, 6, 5671.
12 G. F. Zhang and P. K. Dasgupta, *Anal. Chem.*, **1992**, 64, 517.
13 Y. Xiao, V. Pavlov, T. Niazov, A. Dishon, M. Kotler and I. Willner, *J. Am. Chem. Soc.*, **2004**, 126, 7430.
14 R. Sun, Y. Wang, Y. N. Ni and S. Kokot, *J. Hazard. Mater.*, **2014**, 266, 60.
15 Y. Zhang, Z. Xia, H. Liu, M. J. Yang, L. L. Lin and Q. Z. Li, *Sensor Actuat. B-Chem.*, **2013**, 188, 496.
16 S. Bi, T. T. Zhao, X. Q. Jia and P. He, *Biosens.Bioelectron.*, **2014**,57,110.
17 Y. J. Guo, J. Li and S. J. Dong, *Sensor Actuat. B-Chem.*, **2011**, 160, 295.
18 Y. J. Li, X. Q. Huang, Y. J. Li, Y. X. Xu, Y. Wang, E. B. Zhu, X. F. Duan and Y. Huang, *Sci. Rep.*, **2013**, 3, 1787.
19 S. Y. Deng, J. P. Lei, Y. Huang, Y. Cheng and H. X. Ju, *Anal. Chem.*, **2013**, 85, 5390.
20 R. Frederick, H. Katherine and S. John, *Analyst*, **2009**, 134, 701.
21 F. Tagliaro, C. Poiesi, R. Aiello, R. Dorizzi, S. Ghielmi and M. Marigo, *J. Chromatogr.*, **1993**, 638, 303.
22 T. J. Beveridge, H. R. Smith, S. H. Nader, M. A. Nader and L. J. Porrino, *Neuropharmacology*, **2014**, 85, 528.
23 J. Zhang, L. H. Wang, D. Pan, S. P. Song, F. C. Boey, H. Zhang and C. H. Fan, *Small*, **2008**, 4, 1196.
24 J. L. He, Z. S. Wu, H. Zhou, H. Q. Wang, J. H. Jiang, G. L. Shen and R. Q. Yu, *Anal. Chem.*, **2010**, 82, 1358.
25 C. P. Ma, W. S. Wang, Q. Yang, C. Shi and L. J. Cao, *Biosens. Bioelectron.*, **2011**, 26, 3309.
26 A. V. Azaryan, L. J. Coughlin, B. Buzas, B. J. Clock and B. M. Cox, *J. Neurochem.*, **1996**, 66, 443.
27 L. Qiu, H. Zhou, W. P. Zhu, L. P. Qiu, J. H. Jiang, G. L. Shen and R. Q. Yu, *New J. Chem.*, **2013**, 37, 3998.
28 K. Zhang, K. Wang, X. Zhu, J. Zhang, L. Xu, B. Huang and M. H. Xie, *Chem. Commun.*, **2014**, 50, 180.
29 D. Li, M. B. Muller, S. Gilje, R. B. Kaner and G. G. Wallace, *Nat. Nanotechnol.*, **2008**, 3, 101.
30 F. Liu, and T. S. Seo, *Adv. Funct. Mater.*, **2010**, 20, 1930.
31 A. H. Christopher and K. M. S. Jeremy, *J. Am. Chem. Soc.*, **1990**, 112, 5525.
32 P. G. W. Laurence, *Med. Res. Rev.*, **1986**, 6, 275.
33 J. R. Lupski, J. G. Reid, C. Gonzaga-Jauregui, D. R. Deiros, D. C. Y. Chen, L. Nazareth, et al, *New Engl. J. Med.*, **2010**, 362, 1181.
34 D. T. Miller, Y. Shen, L. A. Weiss, J. Korn, I. Anselm, C. Bridgemohan, G. F. Cox, et al, *J. Med. Genet.*, **2009**, 46, 242.